Supplementary Information: Is Society aware of "Invisible" Droughts? - a Groundwater perspective

Zhenyu Wang[1, 2], Mayra Daniela Peña-Guerrero[2, 3, 4], Jan Sodoge[5], Yanchen Zheng[6, 7], Pia Ebeling[8], Christian Siebert[2], Mariana Madruga de Brito[5, 9], Ralf Merz[2], Kerstin Stahl[10], Wei Zhi[1], Larisa Tarasova[2]

[1] State Key Laboratory of Water Disaster Prevention, Yangtze Institute for Conservation and Development, Hohai University, Nanjing, China

[2] Department Catchment Hydrology, Helmholtz Centre for Environmental Research - UFZ, Halle (Saale), Germany

[3] Humboldt-Universität zu Berlin, Geography Department, Berlin, Germany

[4] Leibniz Institute of Agricultural Development in Transition Economies (IAMO), Halle (Saale), Germany

[5] Department of Urban and Environmental Sociology, Helmholtz Centre for Environmental Research - UFZ, Leipzig, Germany

[6] School of Civil, Aerospace and Design Engineering, University of Bristol, Bristol, UK

[7] School of Geographical Sciences, University of Bristol, Bristol, UK

[8] Department of Hydrogeology, Helmholtz Centre for Environmental Research - UFZ, Leipzig, Germany

[9] Institute for Geography, Leipzig University, Leipzig, Germany

[10] Faculty of Environment and Natural Resources, University of Freiburg, Freiburg, Germany

Supplementary Text S1. Groundwater-level data sources

The groundwater level data were obtained from the water authorities of 14 German federal states: Klimaschutz und Umwelt Berlin (Sen-MVKU), Landesamt für Umwelt Brandenburg (LfU), Landesanstalt für Umwelt Baden-Württemberg (LUBW), Bayerisches Landesamt für Umwelt (LfU), Senatsverwaltung für Mobilität, Verkehr, Hessisches Landesamt für Naturschutz, Umwelt und Geologie (HLNUG), Landesamt für Umwelt, Naturschutz und Geologie Mecklenburg-Vorpommern (LUNG), Landesamt für Natur, Umwelt und Klimaschutz Nordrhein-Westfalen (LANUV), Niedersächsischer Landesbetrieb für Wasserwirtschaft, Küsten- und Naturschutz (NLWKN), Landesamt für Umwelt Rheinland-Pfalz (LfU), Sächsisches Landesamt für Umwelt, Landwirtschaft und Geologie (LfULG), Landesbetrieb für Hochwasserschutz und Wasserwirtschaft Sachsen-Anhalt (LHW), Landesamt für Umwelt- und Arbeitsschutz Saarland (LUA), Landesamt für Umwelt Schleswig-Holstein (LfU), and Thüringer Landesamt für Umwelt, Bergbau und Naturschutz (TLUBN). The original dataset comprised groundwater-level time series from 40,631 monitoring wells (**Table S1**), each with observations available in at least 11 of 12 consecutive months within a calendar year.

The well-specific static data include coordinates standardized to EPSG:25832, ground surface elevation (GOK_NN, m), measuring point elevation (MPH_NN, m), well depth, the top and bottom depths of screens, and near-natural status as provided by the responsible authorities. Wells explicitly identified by the authorities as being under near-natural conditions were flagged as TRUE; all others were flagged as FALSE, indicating only the absence of an explicit near-natural designation rather than confirmed non-near-natural conditions. We also incorporated static hydrogeological characteristics (e.g., aquifer types, hydraulic permeability) obtained from HÜK200 datasets offered by the Federal Institute for Geosciences and Natural Resources (BGR) [1].

Table S1 Number of wells provided by each German federal state and used in this study

States	Datasets	
	Raw	This study
Berlin (B)	443	239
Brandenburg (BR)	1,791	1,139
Baden-Württemberg (BW)	2,959	1,067
Bayern (BY)	566	185
Hessen (H)	1,292	805
Mecklenburg-Vorpommern (MV)	656	171
Nordrhein-Westfalen (NRW)	24,135	7,582
Niedersachsen (NS)	3,015	1,605
Rheinland-Pfalz (RP)	1,008	600
Sachsen (S)	2,246	746
Sachsen-Anhalt (SA)	1,212	454
Saarland (SAAR)	42	12
Schleswig-Holstein (SH)	865	330
Thüringen (TH)	401	120
Total	40,631	15,055

Supplementary Text S2. Groundwater-level data preprocessing

2.1 Data harmonization

As the raw datasets obtained from 14 German state water authorities were generated under different data-management standards, we harmonized them into a unified format. Groundwater-level time series were standardized to a daily temporal resolution. When records from the same well were available from multiple data sources, overlapping observations were compared to identify systematic vertical offsets caused by changes in the measurement reference elevation. When present, the offset was estimated as the median difference between overlapping observations and applied to the newly added record before merging the time series. An IQR-based method [2] was used to exclude potential outliers from the overlapping observations before offset estimation and evaluation. For static information on well depth used for this study, the bottom depth of the screen was prioritized over the reported well depth when both were available, as it provides a more representative indication of the depth from which groundwater enters the well. Invalid or missing values of well depth,

including −999, 0, and unavailable records, were checked and consistently assigned as missing values (NA).

2.2 Data quality check

Groundwater-level time series were subjected to a systematic quality-control procedure to fill short data gaps and identify outliers, abrupt level shifts, prolonged constant values, missing-data periods, and isolated measurements. The details were as follows:

Filling data gaps (Fig. S1): Before quality assessment, short data gaps were linearly interpolated using the Python package SciPy to facilitate the application of anomaly-detection algorithms. Interpolation was restricted to gaps of up to 45 days, while longer gaps remained missing and were flagged as SUSPECT. The 45-day threshold was selected because measurements collected at monthly intervals were not always made on the same calendar day, resulting in intervals slightly longer than one month between consecutive observations.

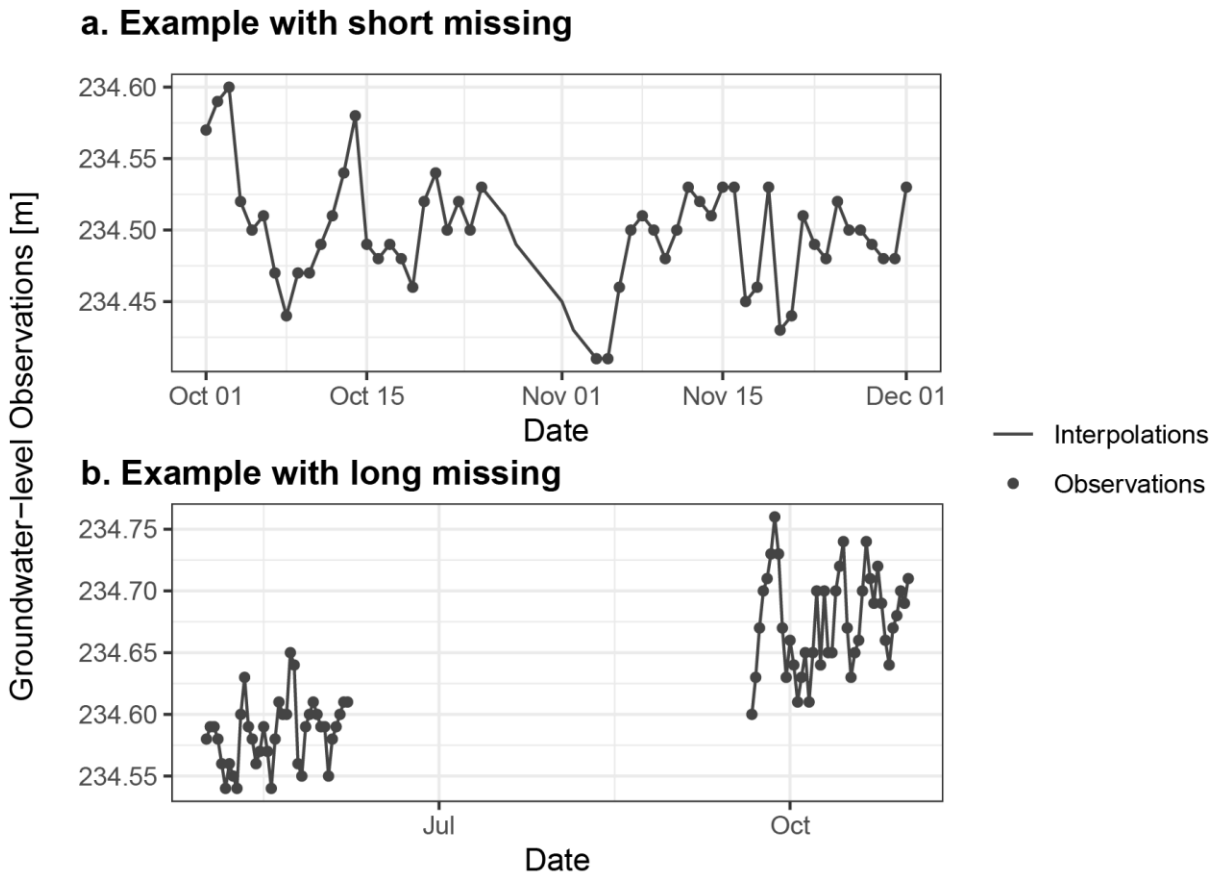


Figure S1 Examples of time series segments with short **(a)** and long **(b)** missing-data gaps.

Identifying constants (Fig. S2): Prolonged periods of nearly constant groundwater levels were identified using the Python package SaQC and flagged as **SUSPECT** when variations remained below 0.001 m within a 183-day (approximately half-year) moving window.

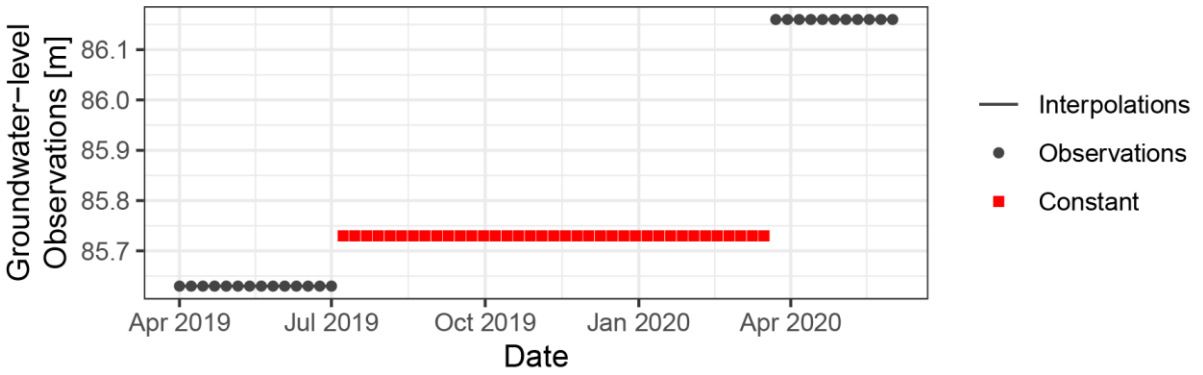


Figure S2 Examples of time series segments with constants.

Identifying outliers (Fig. S3): We implemented a multi-criteria outlier-detection approach to robustly identify outliers [3]. Before outlier detection, long-term trends were removed using robust Theil-Sen regression implemented in the Python package scikit-learn.

Global outliers were independently detected from the detrended time series using three complementary methods: the generalized extreme Studentized deviate (ESD) [4] method, Isolation Forest [5], and a global Z-score criterion. For ESD, implemented using the Python package pyculiarity, the maximum proportion of anomalies was set to 0.03, a periodicity of 365 days was specified, and anomalies in both directions were considered. Isolation Forest was implemented using scikit-learn with 100 trees, automatic selection of the number of samples, and a contamination fraction of 0.03. The global Z-score was calculated over the entire detrended time series using the standard Z-score method and a threshold of $|Z|>3$. An observation was classified as a **SUSPECT** global outlier only when at least two of these three methods identified it as outliers.

Local outliers were independently evaluated using a univariate Local Outlier Factor (LOF) [6] and a local Z-score, both implemented within SaQC. LOF was calculated using 50 neighboring observations, a detection threshold of 2, and a kd-tree algorithm [7]. The local Z-score was calculated using the standard Z-score method within a 183-day moving window, with a threshold of $|Z|>3$ and a requirement that at least 90% of observations within the window were available. An observation was classified as a **SUSPECT** local outlier only when both LOF and the local Z-score identified it as outliers.

To reduce the risk of misclassifying true regional groundwater responses as outliers, observations identified as global or local outliers were further evaluated using a neighbor-based spatial consistency check based on Dynamic Time Warping (DTW) [8]. For each target well, neighboring wells were first searched within an adaptive radius ranging from 0.5 to 10 km (**Table S2**), with the aim of identifying approximately five neighboring wells while limiting computational cost. Groundwater-level time series from the target and candidate neighboring wells were interpolated to fill all data gaps and standardized using Z-scores to minimize differences in absolute groundwater levels and variability. DTW was then used to evaluate the overall similarity in groundwater-level dynamics between each target–neighbor pair. Comparisons were

restricted to pairs with less than 10% missing data and an overlapping period exceeding three years, and were performed using Euclidean distance, a symmetric step pattern, and a 365-day Sakoe–Chiba constraint [9] on temporal alignment. Neighboring wells with a relative DTW distance below 0.2 were considered to exhibit similar overall time-series dynamics to the target well and were selected for subsequent outlier validation.

For each selected target–neighbor pair, DTW-aligned observations were further compared at individual time points. The absolute difference between the standardized groundwater levels of the target and neighboring wells was calculated for each aligned observation. A neighboring well was considered to show similar groundwater-level behavior at a given time point when this difference did not exceed the mean + 3 × standard deviations of the alignment differences for that well pair. An observation in the target well was considered consistent with neighboring groundwater responses when at least three selected neighboring wells were available and more than 50% showed similar behavior at the corresponding time point. For global or local outliers meeting this criterion, the **SUSPECT** flag was removed because the apparently anomalous behavior was also observed in surrounding wells. The DTW analysis was implemented using the Python package dtw.

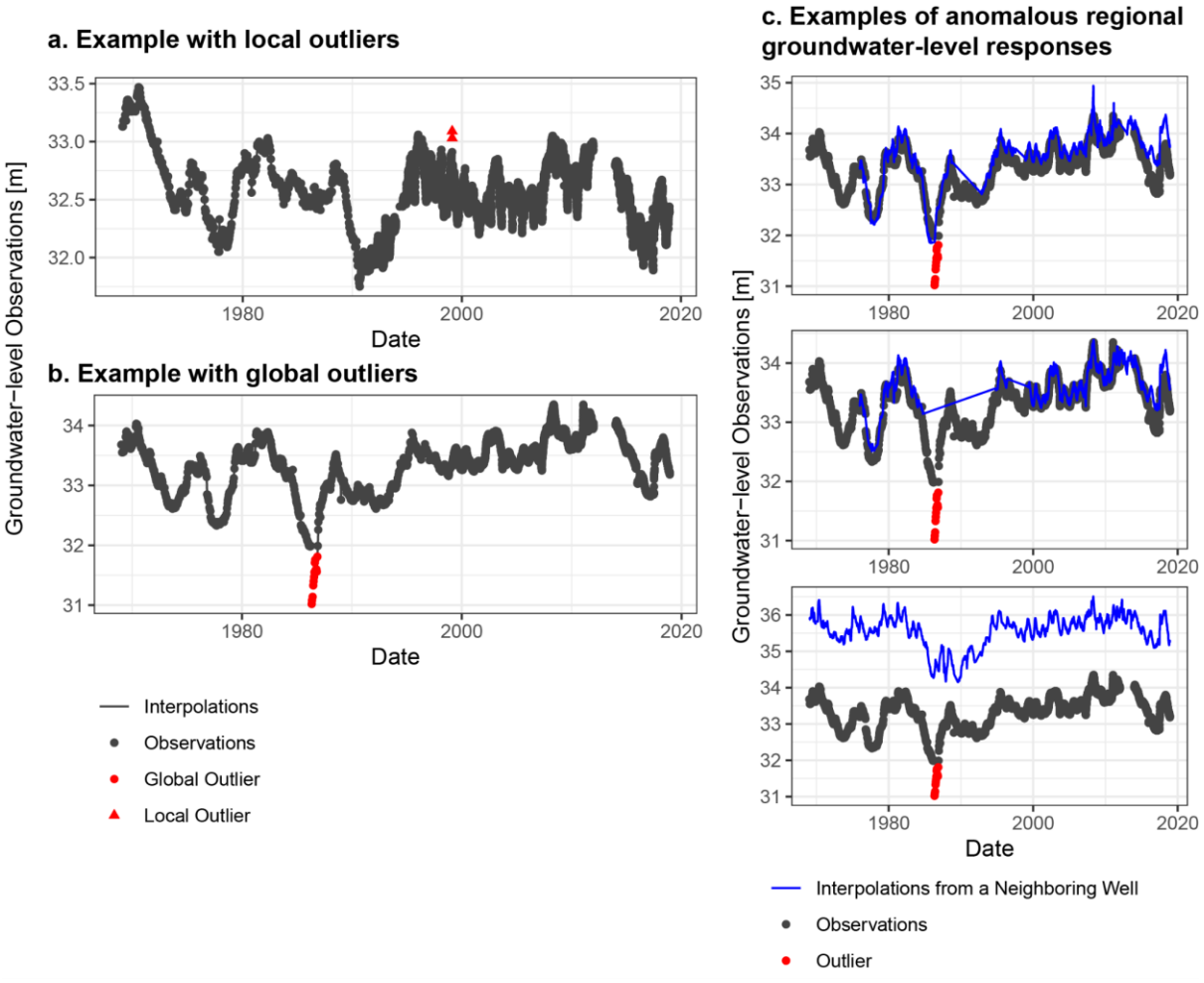


Figure S3 Examples of time-series segments containing local **(a)** and global **(b)** outliers. **c,** Examples of outliers in target wells that coincided with similar groundwater-level responses in

neighboring wells. Black points show observations in the target well, red symbols indicate identified outliers, and blue lines show interpolated groundwater levels from a neighboring well. Similar groundwater-level behavior at the time point of the identified outlier was observed in two of the three neighboring wells that had been identified by DTW as having similar overall time-series dynamics to the target well (upper and lower panels). The identified outlier was, therefore, considered a potentially anomalous regional groundwater-level response rather than a suspect observation.

Table S2 Mean number of neighboring wells within search radius (0.5–10 km) for each federal state. The number of neighboring wells corresponding to the search radius used in this study is highlighted in bold red.

Search Radius [km]	Mean number of neighbouring wells													
	B	BR	BW	BY	H	MV	NRW	NS	RP	S	SA	SAAR	SH	TH
0.5	0.7	0.6	0.9	0.1	0.3	0.8	**7.7**	1.2	1.0	0.8	0.3	0.0	1.2	1.4
1	2.5	0.8	2.7	0.2	0.8	0.9	20.5	1.8	2.3	2.1	0.5	0.2	1.3	2.5
1.5	**5.6**	1.1	**5.1**	0.2	1.7	1.3	36.1	2.4	**5.0**	3.8	1.0	0.2	1.4	3.1
2	9.3	1.7	7.9	0.3	2.9	1.6	54.0	3.0	8.1	**6.0**	1.7	0.4	1.6	3.6
2.5	14.0	2.3	11.2	0.3	**4.6**	1.9	74.3	3.7	12.0	8.5	2.4	0.6	1.9	3.9
3	19.2	3.1	14.7	0.4	6.4	2.3	96.9	**4.7**	16.5	11.4	3.4	0.9	2.3	4.4
3.5	25.7	4.0	18.6	0.5	8.4	2.6	121.2	5.8	21.2	14.5	4.4	0.9	2.9	**5.0**
4	32.8	**5.0**	22.7	0.6	10.8	2.9	147.4	7.1	26.8	18.0	**5.6**	1.0	3.7	5.6
4.5	40.8	6.1	27.1	0.8	13.5	3.3	175.1	8.4	32.4	21.6	6.7	1.2	**4.6**	6.0
5	49.0	7.2	31.8	0.9	16.2	3.7	204.7	10.0	38.2	25.6	8.1	1.4	5.7	6.6
5.5	58.3	8.6	36.8	1.1	19.2	4.2	236.1	11.6	44.6	29.9	9.5	1.7	6.8	7.1
6	68.0	9.8	42.1	1.3	22.5	4.6	269.7	13.4	51.4	34.4	10.9	2.1	8.1	7.7
6.5	78.1	11.1	47.5	1.6	26.1	**5.2**	304.9	15.5	58.1	39.1	12.6	2.4	9.5	8.5
7	89.1	12.6	53.3	1.9	29.6	5.8	341.2	17.7	65.5	43.9	14.2	2.8	10.7	9.2
7.5	100.8	14.3	59.3	2.2	33.7	6.4	378.4	19.7	72.8	49.0	16.1	3.1	12.1	10.0
8	112.6	16.0	65.5	2.5	37.7	7.1	417.3	22.1	80.4	54.1	18.0	3.4	13.9	10.9
8.5	124.8	17.7	71.9	2.9	42.0	7.8	457.2	24.4	88.2	59.5	19.9	3.6	15.5	11.7
9	137.3	19.3	78.3	3.3	46.6	8.7	497.8	27.0	96.4	65.0	22.0	3.9	17.3	12.7
9.5	150.7	21.3	84.8	3.8	51.0	9.6	539.1	29.7	104.9	70.5	24.2	4.0	19.5	14.1
10	164.5	23.2	91.4	**4.3**	55.7	10.3	581.8	32.5	113.6	76.2	26.4	**4.3**	21.4	16.3

Identifying abrupt level shifts (Fig. S4): Abrupt groundwater-level shifts were additionally identified using the LevelShiftAD algorithm from the Python package ADTK, which compares the median groundwater levels in two adjacent 30-day moving time

windows and evaluates whether their absolute difference exceeds Q3+6×IQR. Here, IQR=Q3−Q1, where Q1 and Q3 are the 25th and 75th percentiles, respectively. Level shifts were evaluated only when at least 90% of observations within the window were available.

A detected shift was classified as a positive level shift when groundwater levels increased from the beginning to the end of the shift segment, and as a negative level shift when they decreased. A level shift was further classified as irreversible when no subsequent observations returned to the pre-shift range, that is, when all values after the shift segment remained above (for positive shifts) or below (for negative shifts) all values before the shift segment. Otherwise, the shift was classified as a temporary level shift.

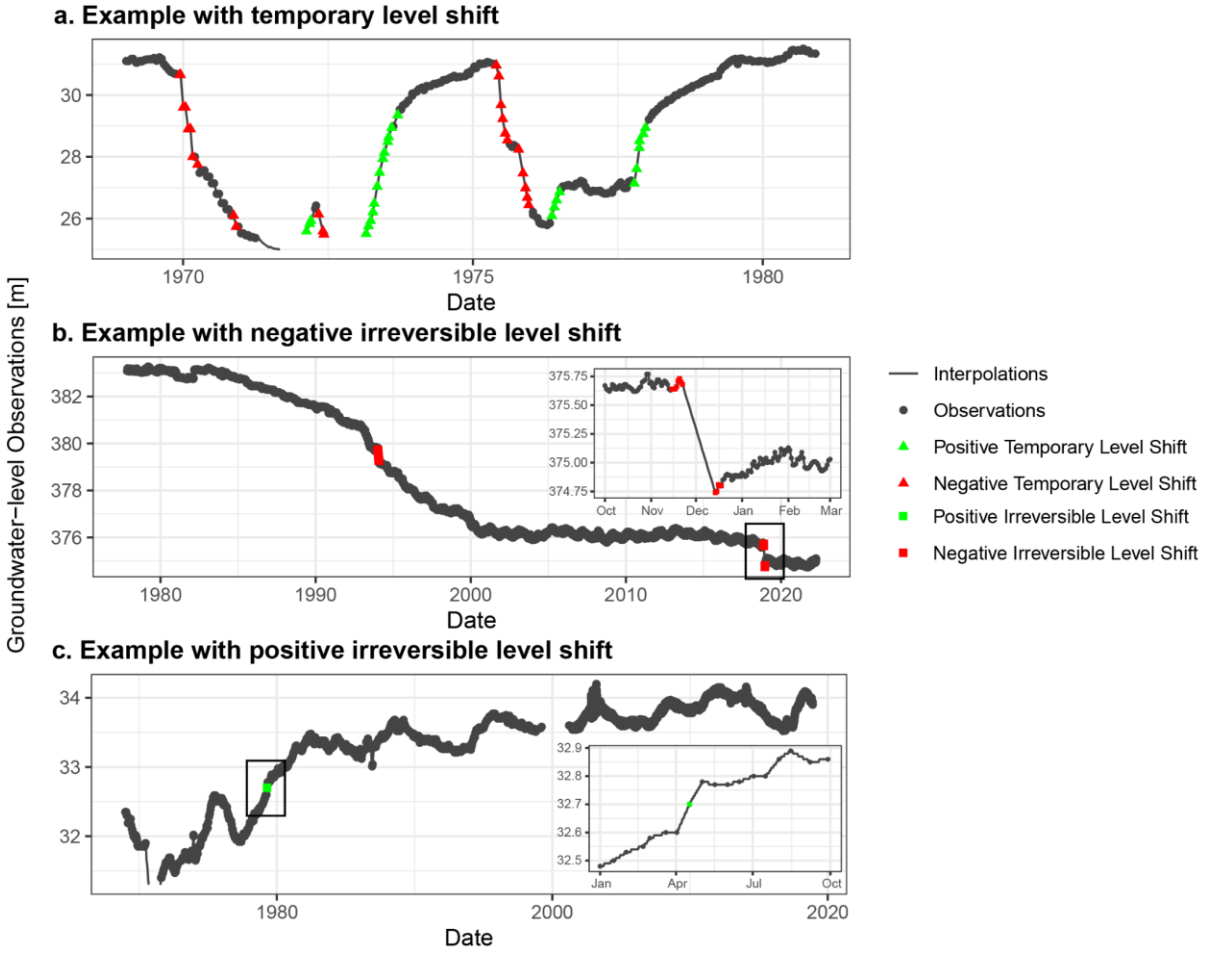


Figure S4 Examples of time series segments with temporary **(a)** and irreversible **(b, c)** level shifts in the direction of positive and negative.

Identifying isolations (Fig. S5): Isolated observations without nearby temporal support within a 30-day window were also flagged as SUSPECT using SaQC.

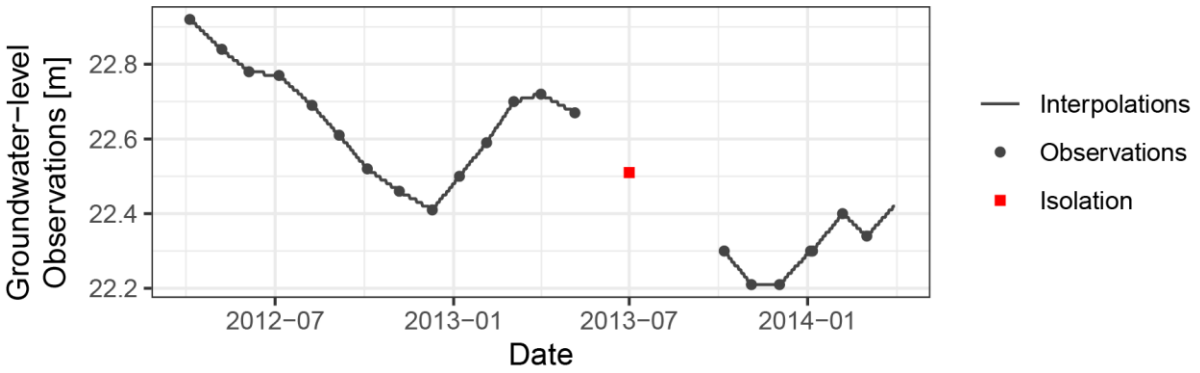


Figure S5 Examples of time series segments with an isolation.

Finally, the SUSPECT datapoints were removed from the raw dataset and filled under the same rules as mentioned above. In addition, 3,302 wells with implausible metadata were excluded from subsequent analyses, retaining only wells with depths between 0 and 500 m. The overall quality-control workflow was integrated and standardized within the package SaQC [10].

Supplementary Text S3. Sensitivity Analysis

As different variable-threshold levels can lead to divergent interpretations of results [11], we conducted a sensitivity analysis using Q80, Q90 and Q95 thresholds and compared the resulting drought characteristics and the number of news reports occurring within identified drought events. As expected, applying more stringent thresholds progressively reduced groundwater drought duration and severity (**Figs. S6a–b**). Relative to Q80, mean drought duration decreased under Q90 by 33.6, 40.5 and 122 days for shallow, intermediate and deep aquifers, respectively, and under Q95 by 61, 110 and 178 days. Mean drought severity showed a similar response, decreasing by 0.06–0.16 m under Q90 and by 0.12–0.42 m under Q95 across aquifer depths.

In contrast to the pronounced changes in drought duration, the number of news reports co-occurring with groundwater drought events changed only modestly (**Fig. S6c**). Relative to Q80, the mean number of co-occurring reports decreased by only 0.3–1.4 under Q90 and 1.3–2.9 under Q95 across aquifer depths. This comparatively limited response is consistent with our finding that societal awareness is only weakly related to groundwater drought duration, providing further evidence of a mismatch between societal awareness and groundwater drought dynamics.

Overall, the increasingly large reductions in drought duration under more stringent thresholds, particularly Q95, indicate that these thresholds increasingly capture the more severe portions of drought events while truncating their broader temporal evolution. We, therefore, retained Q80 as the primary threshold because it better preserves the prolonged groundwater drought dynamics central to our analysis. In addition, the relatively small changes in the number of news reports co-occurring with groundwater drought events between Q80 and Q90 or Q95 demonstrate that our main conclusions regarding the relationship between societal awareness and groundwater drought are robust to the choice of threshold.

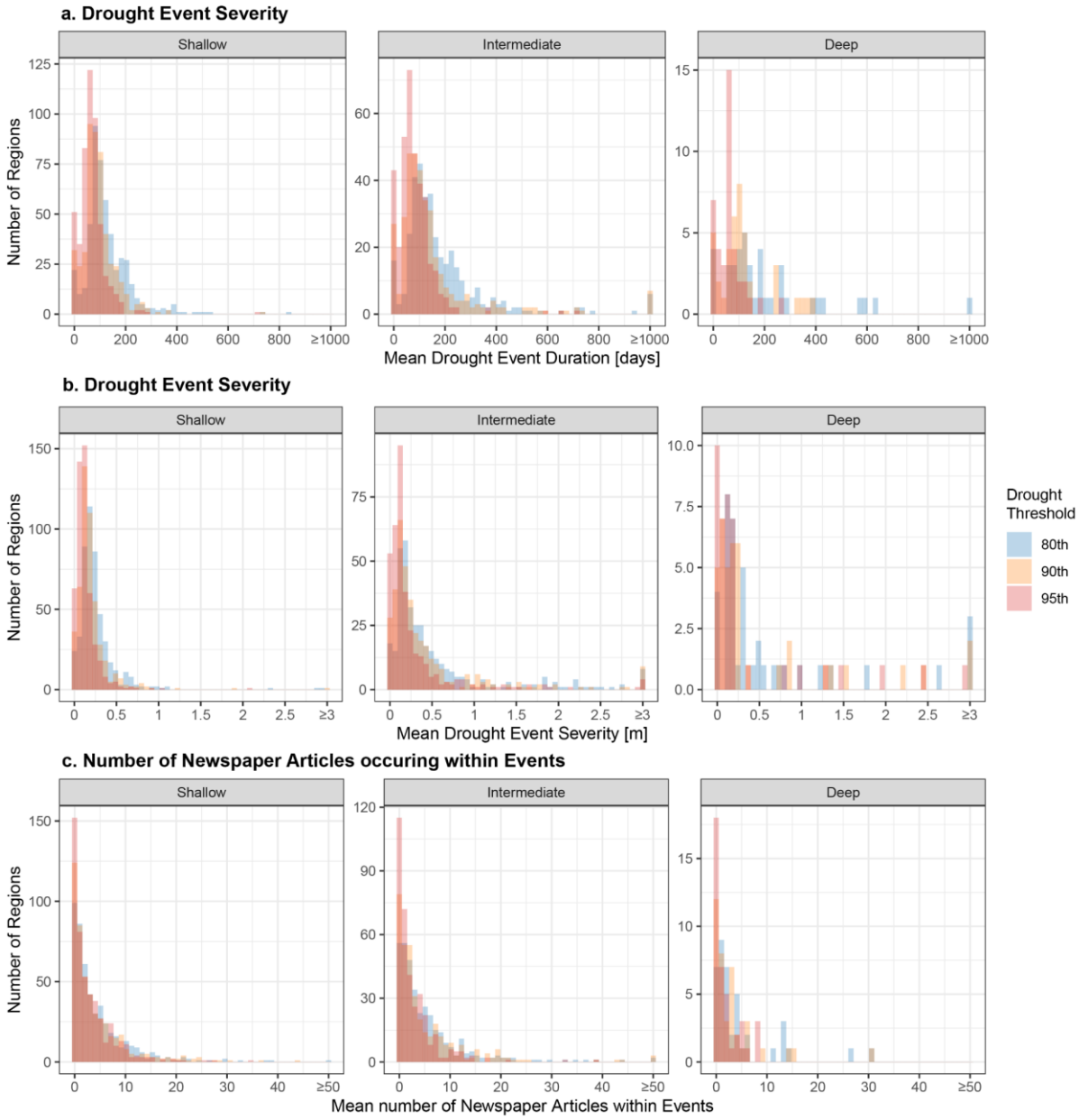


Figure S6 Distributions of regional-specific mean drought event duration **(a)**, severity **(b)**, number of news reports occurring within events **(c)** for variable drought thresholds of Q80, Q90, and Q95.

Supplementary Text S4. Robustness Test of TVR method

We evaluated the robustness of the TVR method through comparison with an independent cross-correlation approach and groundwater-abstraction data. First, we compared TVR with a method based on the cross-correlation between groundwater levels and effective rainfall accumulated over different periods [12]. Among all records, 168 groundwater-level records were independently classified as near-natural by German state authorities (**Fig. S7**). Both methods successfully identified most of these records as being dominated by natural variability, with TVR showing slightly greater agreement with the authority-based classification: 97.6% of the near-natural records had TVR < 1 (**Fig. S8a**), compared with 95.2% having cross-correlation coefficients (ρ) > 0.5 (**Fig. S8b**). Across all wells, 92.0% had TVR < 1, whereas 80.5% had ρ >

0.5. Accordingly, TVR ≥ 1 classified only 8.0% of records as potentially strongly influenced by non-climatic factors, much fewer than the proportion classified by ρ ≤ 0.5. It indicates the TVR threshold provides a more conservative criterion for identifying strong human influence.

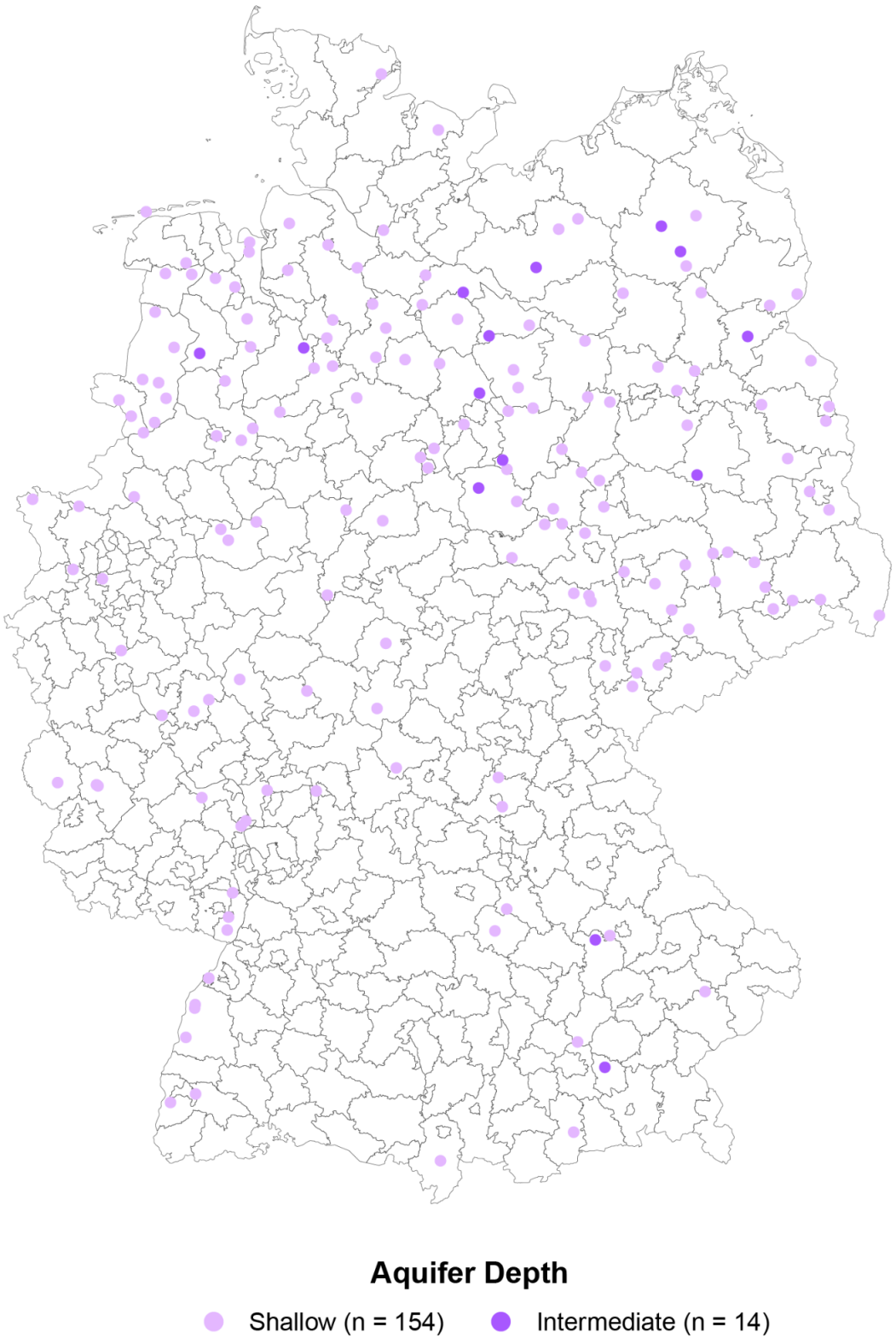


Figure S7 Distribution of 168 near-natural groundwater wells categorized into shallow (0–30 m) and intermediate (30–200 m) aquifers based on well depth. Each area outlined with a solid line represents a German administrative region at the third level of the Nomenclature of Territorial Units for Statistics (NUTS3).

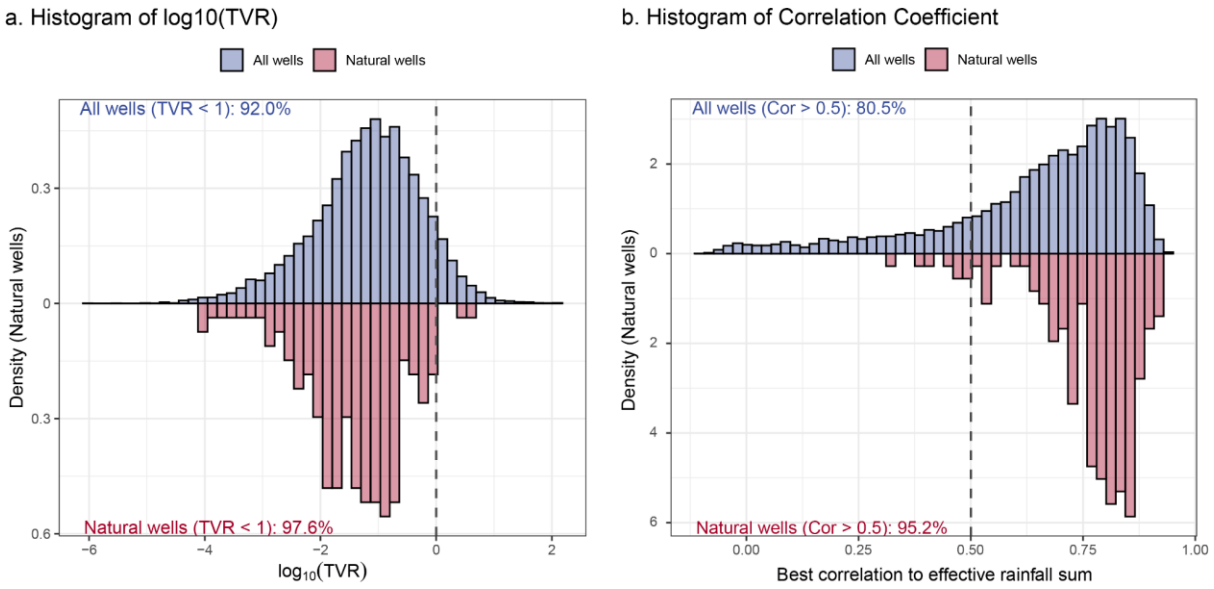


Figure S8 Evaluation of criteria for identifying strong human influences on groundwater levels. Upper and lower panels show distributions for all wells and for near-natural wells identified by the responsible authorities, respectively. **a,** Distribution of the log10-transformed trend-to-variability ratio (TVR). The dashed line at log10(TVR) = 0 (TVR = 1) indicates the threshold used to identify groundwater-level records with strong long-term human influences. **b,** Distribution of the maximum correlation coefficient (ρ) between groundwater level and effective rainfall at the optimal accumulation period and lag time. Effective rainfall was calculated as precipitation minus modified-Hargreaves-estimated potential evapotranspiration [13] using HYRAS meteorological data available from the German Weather Service (DWD) [14]. The dashed line at ρ = 0.5 indicates the threshold used to distinguish groundwater-level records strongly coupled to climatic forcing from those with weaker coupling.

Second, we compared the classifications obtained from the two methods across all groundwater-level records. Overall, 79.7% showed consistent classifications, with either TVR < 1 and ρ > 0.5 or TVR ≥ 1 and ρ ≤ 0.5 (**Fig. S9**), indicating broad agreement between TVR and the degree to which groundwater dynamics are coupled to climatic recharge. A further 15.7% of records had TVR < 1 but ρ ≤ 0.5, consistent with the more conservative classification obtained using TVR ≥ 1. It may, therefore, underestimate the extent to which human or other non-recharge factors affect groundwater dynamics.

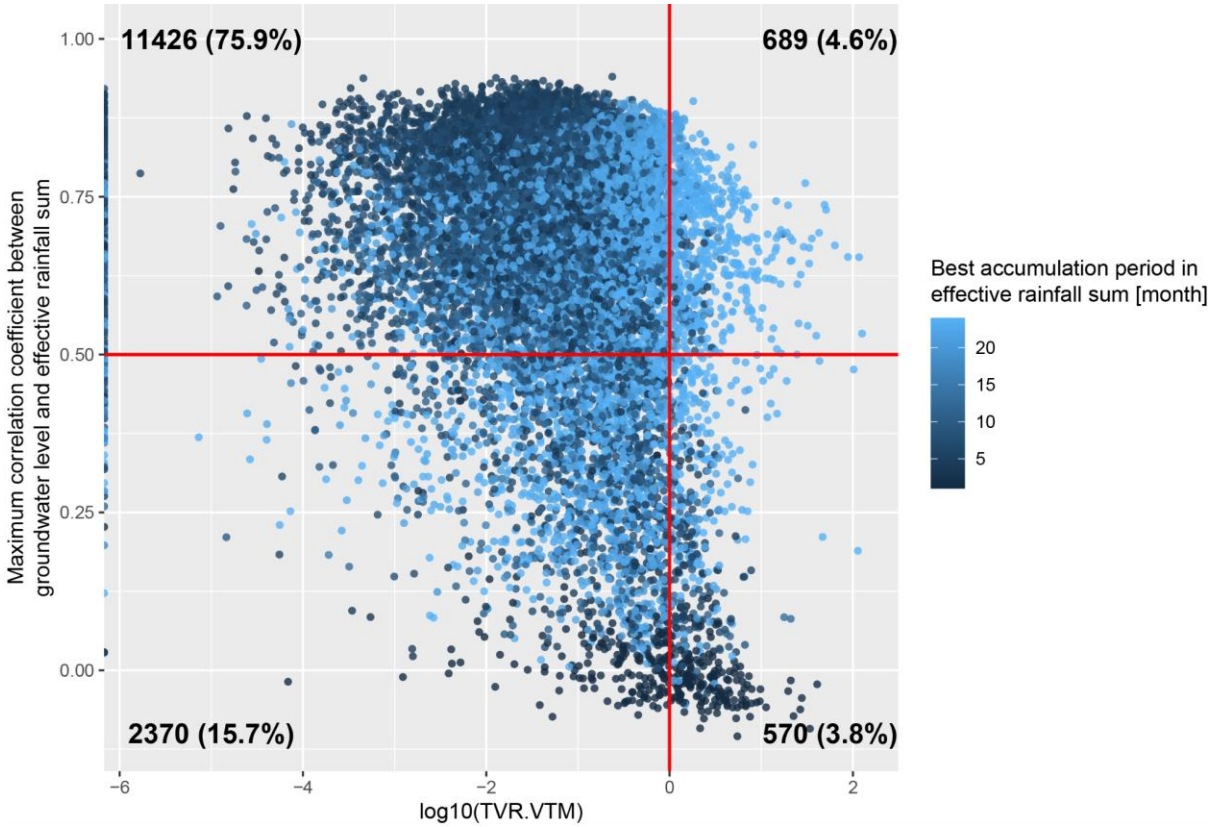


Figure S9 Comparison between the log10-transformed trend-to-variability ratio (TVR) and the maximum correlation coefficient between groundwater level and effective rainfall accumulated over the optimal accumulation period and lag time. Point colour indicates the optimal accumulation period.

Finally, we independently evaluated TVR against groundwater-abstraction data in the UK. Groundwater-level records with TVR ≥ 1 were spatially concentrated in regions with high groundwater abstraction (>1 × 10^8 m^3; **Fig. S10**), providing further evidence that high TVR values capture strong human influences on groundwater dynamics. Together, these independent evaluations support the robustness of TVR as a conservative indicator of strong human influences on groundwater levels.

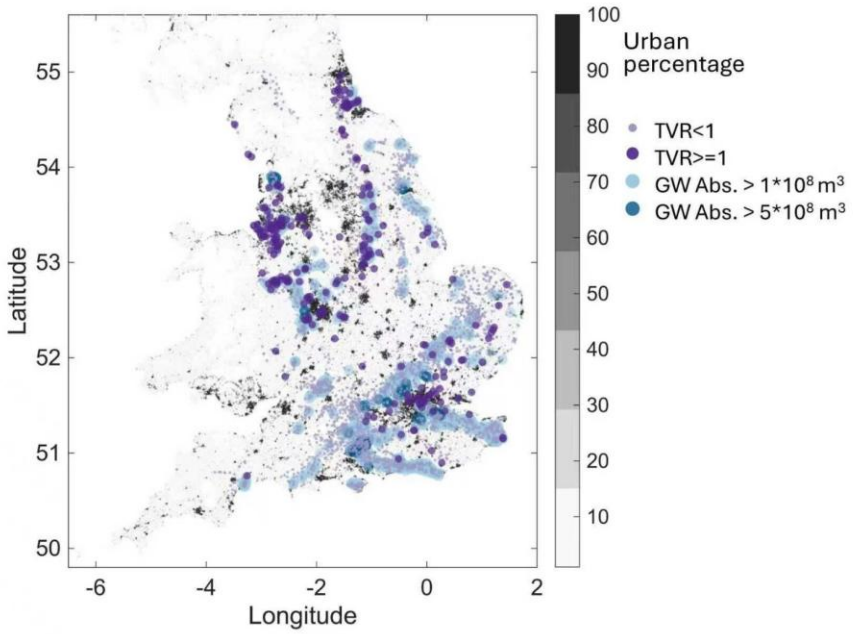
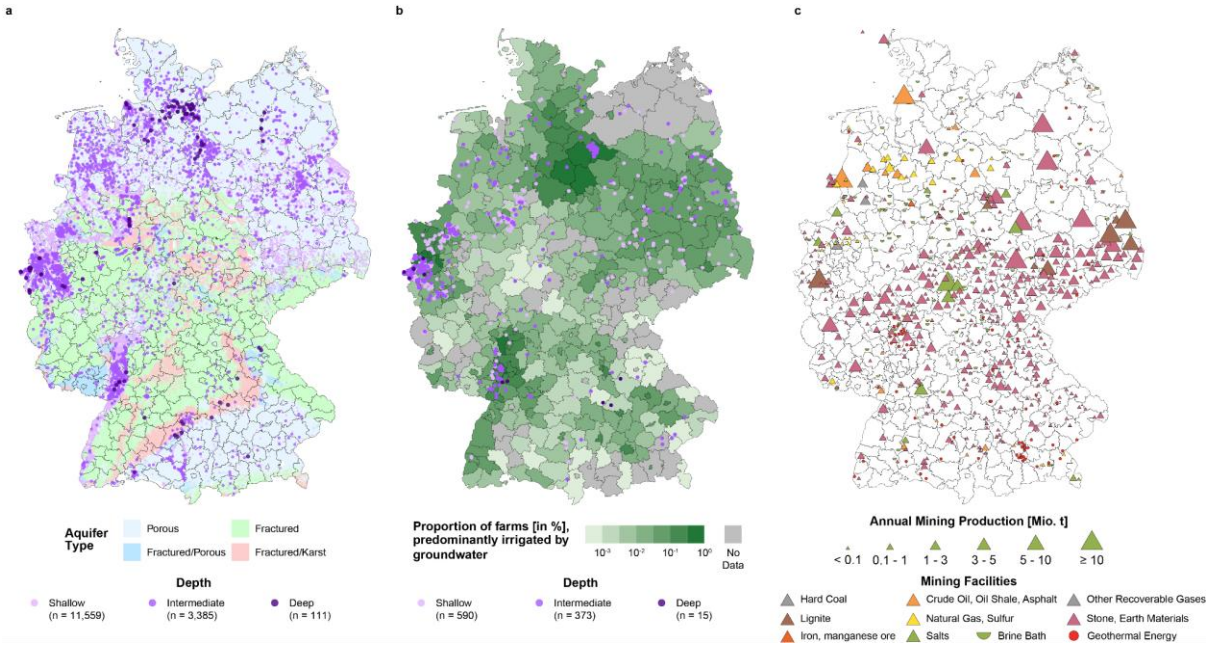
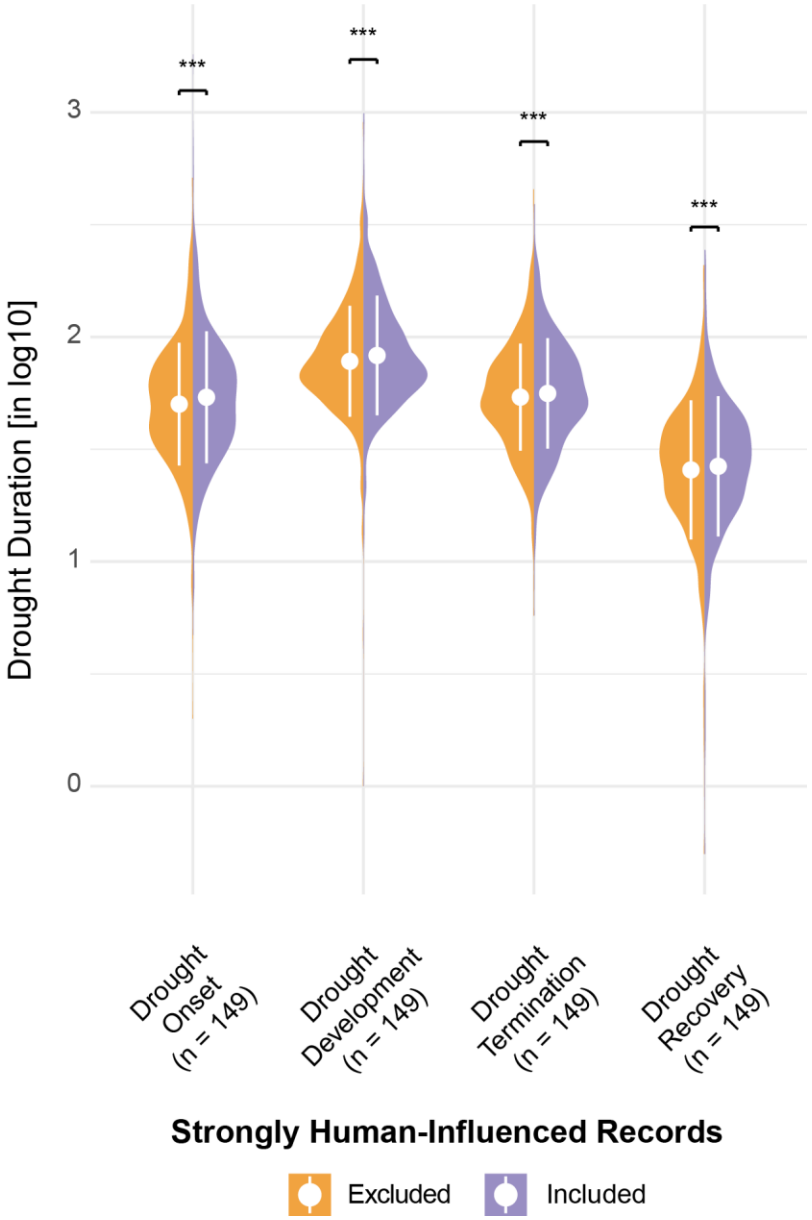


Figure S10 Application of the TVR method in the UK. Purple points represent groundwater wells, with darker purple indicating wells with TVR ≥ 1. Blue points represent groundwater abstraction monitoring sites, with darker blue indicating abstraction volumes > 5 × 10^8 m³. Wells with TVR ≥ 1 are mostly located near regions with high groundwater abstraction, supporting the ability of the TVR method to distinguish groundwater systems potentially influenced by human activities.

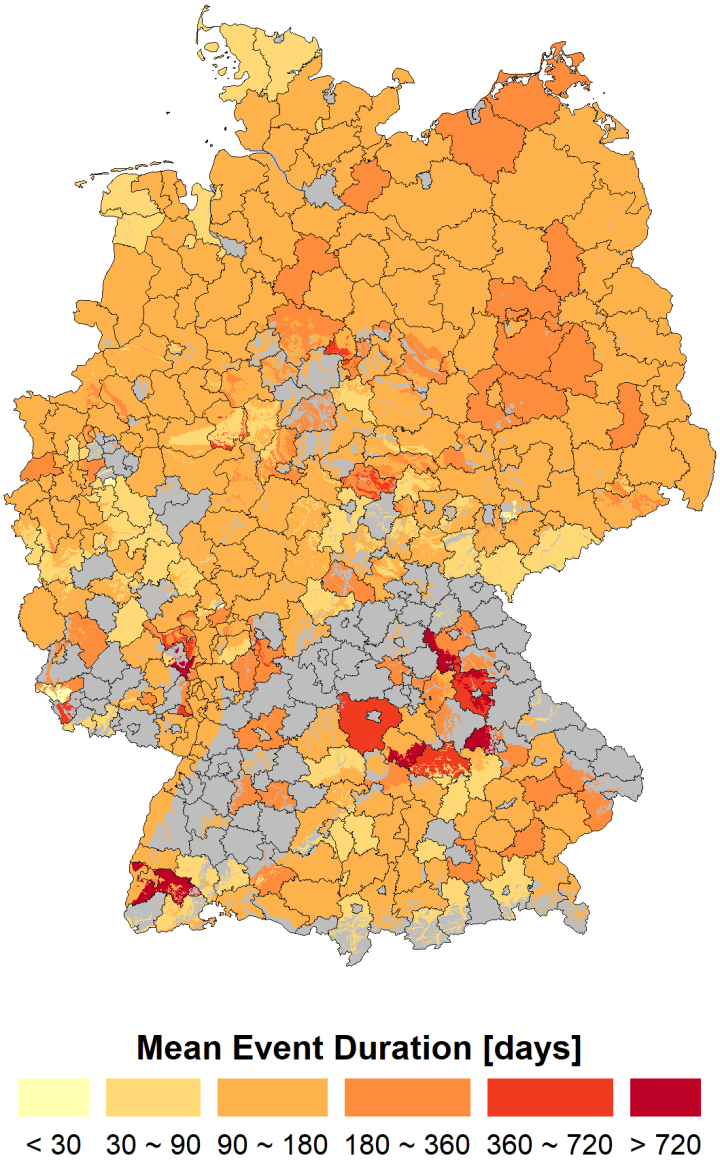
Supplementary Figures



Extended Figure 1 Distribution of groundwater wells and groundwater-related human activities in Germany. a, Distribution of groundwater wells categorized into shallow (0–30 m), intermediate (30–200 m), and deep (200–500 m) aquifers based on well depth. Each area outlined with a solid line represents a German administrative region at the third level of the Nomenclature of Territorial Units for Statistics (NUTS3). The background colors represent different aquifer types [1]. **b,** Distribution of wells with strong human influences. Points mark wells containing strongly human-influenced records, defined as those exhibiting pronounced long-term trends or irreversible level shifts before an event, across three aquifer depth classes. Areas in green show the proportion of farms predominantly using nearby groundwater (also spring water and bank filtrate) sources for irrigation (%) in NUTS-3 level [15]. **c,** Distribution of mining facilities provided by the Federal Institute for Geosciences and Natural Resources (BGR) [16]. Point size represents annual mining production, while colour and symbol shape indicate facility type.



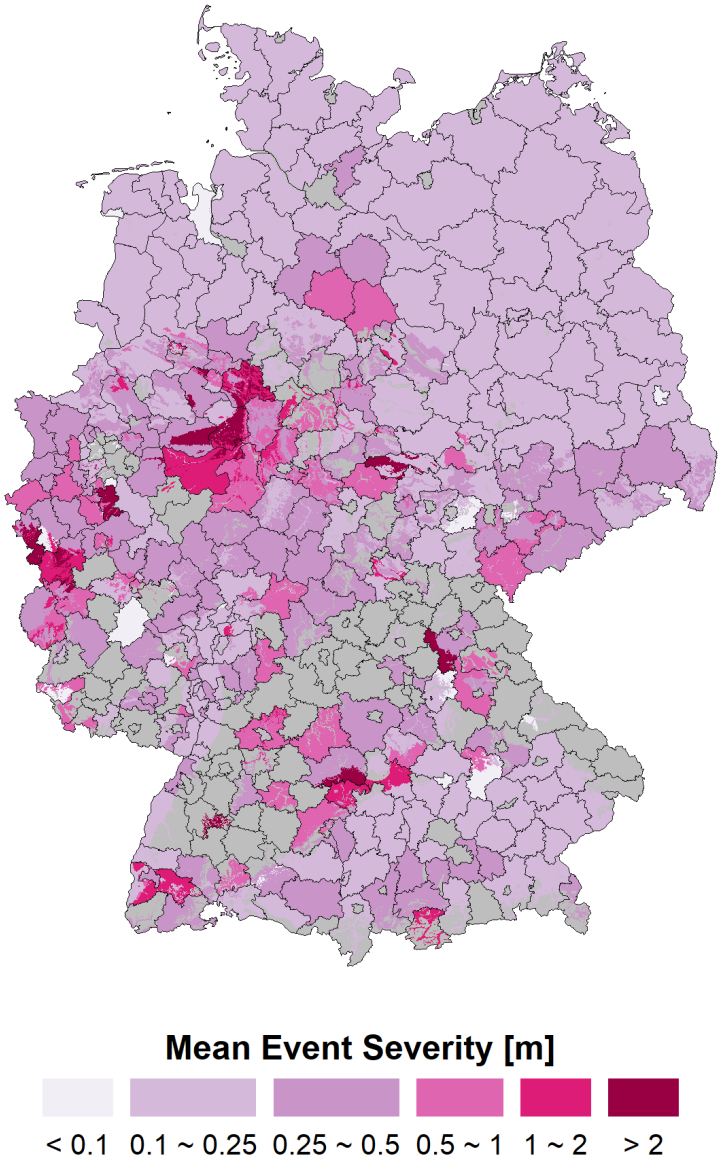
Extended Figure 2 Violin plots of duration for each phase across drought phases when excluding (left; orange) and including (right; purple) strongly human-influenced records. The analysis included 149 regions with comparable records with and without strong human influences. White dots and error bars show mean ± s.d. Differences between drought characteristics were tested using paired Wilcoxon signed-rank tests (*: $P < 0.05$; **: $P < 0.01$; ***: $P < 0.001$; ns: not significant). The strong human impacts extend the onset, development, termination, and recovery phases by 16.6, 29.3, 7.9, and 3.9 days.



278

279 **Extended Figure 3** Spatial distribution of region-specific mean drought duration in Germany
280 based on all records. Regions in grey mean no data available. The overall mean event duration
281 (± standard deviation) is 152.0 ± 159.9 days.

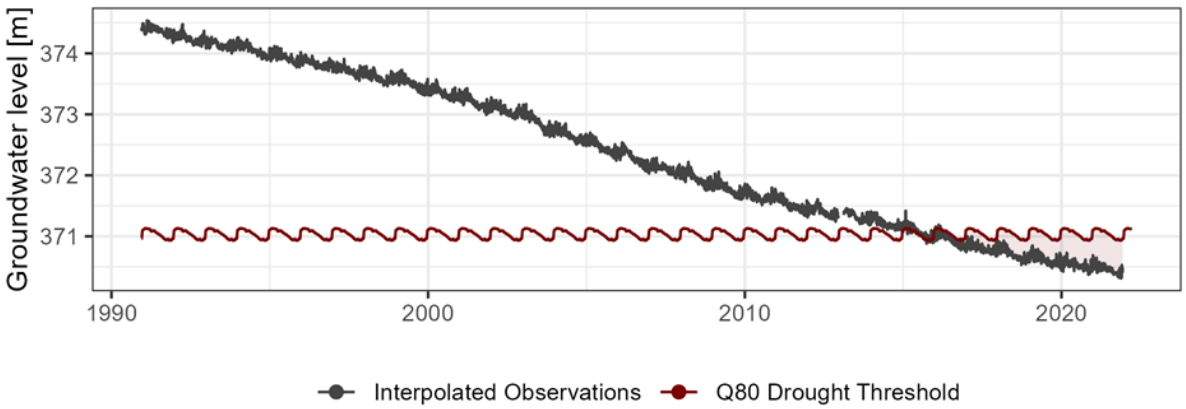
282



283

284 **Extended Figure 4** Spatial distribution of region-specific mean drought severity (i.e., the
285 maximum deviation below the drought threshold) in Germany based on all records. Regions
286 in grey mean no data available. The overall mean event severity (± standard deviation) is 0.44
287 ± 0.65 m.

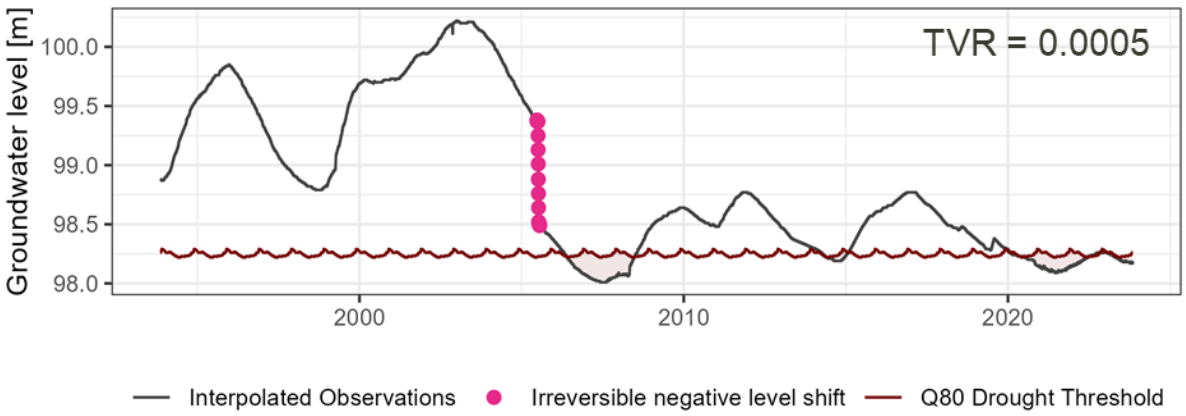
288



289

290 **Extended Figure 5** An example of a groundwater-level record with TVR ≥ 1 (TVR = 125.81)

291



292

293 **Extended Figure 6** An example of a groundwater-level record with a segment containing at
294 least one event that includes or occurs after an irreversible level shift (TVR = 0.0005).

295

Reference

1. BGR. Hydrogeologische Übersichtskarte von Deutschland 1:200.000 (HÜK200).
2. Rousseeuw, P. J. & Hubert, M. Robust statistics for outlier detection. *WIREs Data Min. Knowl. Discov.* **1**, 73–79 (2011).
3. Ohmer, M. *et al.* GEMS-GER: a machine learning benchmark dataset of long-term groundwater levels in Germany with meteorological forcings and site-specific environmental features. *Earth Syst Sci Data* **18**, 77–95 (2026).
4. Rosner, B. Percentage Points for a Generalized ESD Many-Outlier Procedure. *Technometrics* **25**, 165–172 (1983).
5. Liu, F. T., Ting, K. M. & Zhou, Z.-H. Isolation-based anomaly detection. *ACM Trans. Knowl. Discov. Data TKDD* **6**, 1–39 (2012).
6. Breunig, M. M., Kriegel, H.-P., Ng, R. T. & Sander, J. LOF: identifying density-based local outliers. in *Proceedings of the 2000 ACM SIGMOD international conference on Management of data* 93–104 (2000).
7. Friedman, J. H., Bentley, J. L. & Finkel, R. A. An algorithm for finding best matches in logarithmic expected time. *ACM Trans. Math. Softw. TOMS* **3**, 209–226 (1977).
8. Rinderer, M., McGlynn, B. L. & van Meerveld, H. J. Groundwater similarity across a watershed derived from time-warped and flow-corrected time series. *Water Resour. Res.* **53**, 3921–3940 (2017).
9. Geler, Z., Kurbalija, V., Ivanović, M. & Radovanović, M. Elastic distances for time-series classification: Itakura versus Sakoe-Chiba constraints. *Knowl. Inf. Syst.* **64**, 2797–2832 (2022).
10. Schmidt, L. *et al.* System for automated Quality Control (SaQC) to enable traceable and reproducible data streams in environmental science. *Environ. Model. Softw.* **169**, 105809 (2023).
11. Heudorfer, B. & Stahl, K. Comparison of different threshold level methods for drought propagation analysis in Germany. *Hydrol. Res.* **48**, 1311–1326 (2016).

12. Baulon, L., Massei, N., Allier, D., Fournier, M. & Bessiere, H. Influence of low-frequency variability on high and low groundwater levels: example of aquifers in the Paris Basin. *Hydrol Earth Syst Sci* **26**, 2829–2854 (2022).

13. Droogers, P. & Allen, R. G. Estimating Reference Evapotranspiration Under Inaccurate Data Conditions. *Irrig. Drain. Syst.* **16**, 33–45 (2002).

14. DWD. Hydrometeorologische Rasterdaten. https://opendata.dwd.de/climate_environment/CDC/.

15. Bernhardt, J. J. & Neuenfeldt, S. Spatial Data on Irrigation in Germany: A Comprehensive Analysis of Agricultural Statistical Data the NUTS-3 Level for the Years 2009 and 2019. OpenAgrar https://doi.org/10.3220/DATA20241120161738-0 (2024).

16. BGR. Karte der Bergbau- und Speicherbetriebe 1 : 2 000 000 (BergSP). https://www.bgr.bund.de/DE/BGR/Wissenschaftliche-Infrastruktur/Geologie-Bohrungen/Karten/Deutschland/Kt_Bergbau/bergSP_inhalt.html (2026).